Temperature-pressure phase diagram of URu_2Si_2 from resistivity measurements and ac calorimetry: Hidden order and Fermi-surface nesting

E. Hassinger,* G. Knebel, K. Izawa, P. Lejay, B. Salce, and J. Flouquet
Département de Recherche Fondamentale sur la Matière Condensée, SPSMS/CEA Grenoble, 17 rue des Martyrs, 38054 Grenoble Cedex 9, France

(Received 29 August 2007; revised manuscript received 19 December 2007; published 12 March 2008)

By performing combined resistivity and calorimetric experiments under pressure, we have determined a precise temperature-pressure (T,P) phase diagram of the heavy fermion compound URu_2Si_2. It will be compared with previous diagrams determined by elastic neutron diffraction and strain gauge techniques. At first glance, the low-pressure ordered phase referred to as hidden order is dominated by Fermi-surface nesting, which has strong consequences on the localized spin dynamics. The high-pressure phase is dominated by large moment antiferromagnetism (LMAF) coexisting with at least dynamical nesting needed to restore on cooling a local moment behavior. ac calorimetry confirms unambiguously that bulk superconductivity does not coexist with LMAF. URu_2Si_2 is one of the most spectacular examples of the dual itinerant and local character of uranium-based heavy fermion compounds.

DOI: 10.1103/PhysRevB.77.115117 PACS number(s): 71.27.+a, 74.70.Tx, 75.30.Mb

I. INTRODUCTION

The heavy fermion compound URu_2Si_2 has attracted much attention mainly due to the observation of a tiny antiferromagnetically ordered moment $M_0 \sim 0.03\mu_B$ at $T \to 0$ K with wave vector $Q_0=(1,0,0)$.[1] However, M_0 is too weak to be the origin of the large anomaly associated with the ordering temperature $T_0=17.5$ K, which implies that the ordered state is not that of a classical antiferromagnet (AF). Different theoretical models have been proposed to account for the loss of entropy at the transition such as the formation of a spin or charge-density wave, which may be coupled with another antiferromagnetic component,[2] higher orbital ordering,[3–5] "orbital antiferromagnetism,"[6] or "helicity order."[7] However, large changes in the inelastic spin excitation spectrum have been observed in neutron scattering experiments and agree with the size of the specific heat anomaly.[8,9] The fluctuations at the commensurate wave vector $Q_0=(1,0,0)$ are associated with an energy $E_0 \sim 2.1$ meV and are characteristic of a gapped energy spectrum that opens just below T_0. Another gapped energy spectrum with a similar intensity appears at an incommensurate wave vector $Q_1=(1.4,0,0)$ below T_0.[3,10,11] In contrast to the Q_0 case, no sublattice magnetization can be detected at Q_1. Looking now to the charge motion by electrical and thermal transport,[12–15] the main phenomenon at T_0 is the opening of a partial gap Δ_G at the Fermi level and the decrease of the carrier number is estimated to be by a factor of 3–10. The debate on the possible ground state for URu_2Si_2 at ambient pressure (P) has involved different possibilities (for a recent overview, see also Ref. 16). However, the fact that the major phenomenon at T_0 is certainly the drop in the carrier number has frequently been omitted. The uncertainty in the exact nature of the order parameter below T_0 has led to the low-temperature–low-pressure phase of URu_2Si_2 being denoted as hidden order (HO).

New insight into the understanding of the ground-state properties of URu_2Si_2 came from a high-pressure neutron diffraction scattering study which claims a transition from the HO state to large moment antiferromagnetism (LMAF) with M_0 reaching $0.3\mu_B$ above 1 GPa.[17] Further, with strain gauge experiments a transition has been detected at $P_x \sim 0.5$ GPa for $T \to 0$ K. The transition was claimed to be of first order. Above 1.3 GPa a single transition occurs from a paramagnetic (PM) state to LMAF on cooling.[18] Successive neutron diffraction experiments indicate that LMAF is the ground state of URu_2Si_2 above P_x.[16,19] Furthermore, it seems now that there is a consensus by NMR,[20,21] muon spectroscopy,[22] and neutron scattering[16] that a pure HO ground state below P_x will exclude tiny ordered moments M_0 at Q_0.

The aim of this paper is to draw carefully the (T,P) phase diagram of URu_2Si_2 in excellent hydrostatic conditions by combining resistivity measurements [highly sensitive to the nesting of the Fermi surface (FS)] and calorimetric experiments (a good technique to qualify the bulk nature of a phase transition). Special attention has been paid to small P variations. One goal was especially to detect if the transition line between the HO phase and the LMAF phase $T_x(P)$ ends in a critical end point or if it unites with the initial transition line between the PM and the HO phase $T_0(P)$ at some tricritical point (T^*,P^*), leading to a single line $T_N(P)$ at higher pressures. A phenomenological model predicts that the $T_x(P)$ line may end in a critical end point (case A) if there is a coexistence of two orderings with the same antiferromagnetic dipole symmetry, while for a different symmetry (case B), the lines $T_0(P)$, $T_x(P)$, and $T_N(P)$ intersect at a tricritical point.[2]

A supplementary interest of URu_2Si_2 is that, in its HO phase, superconductivity (SC) appears below $T_C \sim 1.2$ K, presumably of an unconventional nature.[23] We focus here on the domain of the existence of SC in the HO or LMAF phase. Experimentally, the difficulty to study SC is its high sensitivity to imperfections.[24,25] We observed a drastic difference on the pressure dependence of T_C detected by resistivity (a surface sensitive technique) and specific heat (a bulk probe).

II. EXPERIMENTAL DETAILS

A single crystal of URu_2Si_2 was grown by the Czochralski method in a tri-arc furnace under purified argon atmosphere using uranium (3N: 99.9% purity), ruthenium (4N: 99.99% purity), and silicon (6N: 99.9999% purity) as starting materials. The crystal was prepared under the same experimental conditions as those already used in Grenoble for the study of SC,[26] of neutron scattering,[27] and of quantum oscillations in Cambridge[28] or Tallahassee.[29] Large single crystals of centimeter size have been obtained as verified by neutron scattering.[27] The crystal is pulled at about 5 mm/h. A rotation of about 20 turns per minute homogenizes the temperature during the growing process. A large single crystal of 5 mm in diameter and of several centimeters in length in the direction of the crystalline c axis has been obtained. The large single crystal was cut, using electroerosion, into different pieces with masses of about 1 mg which have been tested by specific heat measurements in a Quantum Design PPMS. The final sample for the high-pressure measurements (denoted as sample 2b) has been prepared from the one of these samples (denoted as sample 2) showing the steepest superconducting transition in the specific heat. The width of the superconducting transition (ΔT_c=0.15 K in the resistivity at ambient pressure) is comparable to that of the best sample in Ref. 24.

Figure 1(a) shows the temperature dependence of the specific heat and the resistivity of sample 2 close to the transition at T_0. The transition temperature T_0 in the specific heat is defined by the maximum of C/T. This temperature corresponds to the minimum of the temperature derivative of the resistivity curve. The superconducting transition of sample 2 is shown in Fig. 1(b). The transition to the superconducting state does not appear at the same temperature in specific heat and resistivity measurements; in the specific heat the transition occurs when the resistivity is already zero. The ac susceptibility measurement clearly shows a structure in the superconducting transition. Similar shifts of the transition temperatures were always observed on all published data when such a comparison has been performed.[24,25] At least for URu_2Si_2, the curious phenomenon is that, by annealing, the SC specific heat anomaly can become sharper than the ones detected by resistivity and susceptibility.[30] This is in strong contrast to the data obtained on UPt_3 superconductors.

The sample for the high-pressure measurements was cut from this sample 2 with a circular saw. The thickness was reduced by polishing with a diamond coated disc. The final size of the parallelepiped sample was $283\times60\times50$ μm^3. Laue diffraction showed that the long axis of this sample was misaligned in polar coordinates ϕ=7° and θ=25° with respect to the tetragonal c axis. For resistivity and specific heat experiments the same sample has been used. The resistivity was measured using a standard four point lock-in technique. Electrical contacts to the sample have been realized by spot welding 10 or 12 μm Au wires to the sample. A current of 100 μA was used to measure the resistivity. The specific heat has been measured by a specially developed ac calorimetric technique.[31,32] At low temperatures, the laser beam of a laser diode, which is tunable in frequency and power, and at high temperature ($T>1.5$ K) a mechanically chopped laser beam has been used to heat the sample. The temperature oscillations of the sample were measured with a **Au/AuFe**(0.07%) thermocouple which was directly soldered onto the sample. At low temperatures ($T<2$ K) the measurement frequency was 127 Hz, at higher temperatures 678 Hz. Due to the unknown addenda contribution to the observed signal, this method gives only qualitative information on the specific heat.

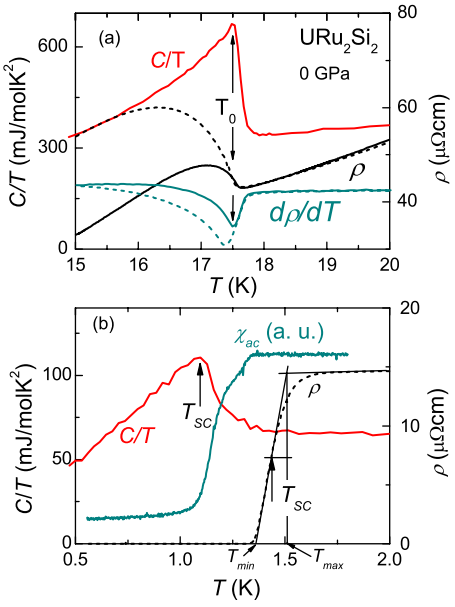

FIG. 1. (Color online) (a) Temperature dependence of the specific heat (red line) and the electrical resistivity of sample 2 at ambient pressure around the phase transition to the HO state at T_0. In the resistivity T_0 is defined by the minimum of the derivative $d\rho/dT$. The dashed line gives the resistivity normalized to the resistivity of sample 2 at T_0 of the small sample inside the uncharged pressure cell. The difference in the resistivity is due to the different orientation of the current injection. For the sample 2(b) in the pressure cell the misalignment is about 25°. (b) Superconducting transition of the initial sample 2 (specific heat and ac susceptibility) and of sample 2(b) inside the uncharged pressure cell (detected by resistivity).

The high-pressure experiments have been performed using an argon loaded diamond anvil pressure cell. Argon guarantees very good hydrostatic pressure conditions. The pressure is determined by the fluorescence of several ruby grains (located at different places in the pressure chamber) at 4.2 K before and after the measurement. No change of pressure due to long time relaxation processes could be observed. The absolute error in pressure is estimated to be about $\Delta P \approx 0.05$ GPa, but the relative error bar is far lower.

Precise pressure-dependent measurements with fine-tuned pressure steps above T=1.5 K have been performed in a ^{4}He cryostat where it is possible to change pressure *in situ* at low temperatures.[33] In this case the pressure inhomogeneity is approximately 10% of the absolute pressure, i.e., 0.05 GPa at the pressure $P_x \approx 0.5$ GPa.

For more detailed measurements at a fixed pressure we used a ^{3}He cryostat to measure resistivity and specific heat in the temperature range from 0.5 K up to 30 K and in mag-

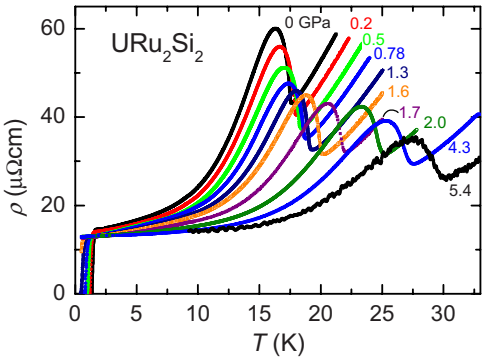

FIG. 2. (Color online) Temperature dependence of the resistivity of URu_2Si_2 for different pressures from $P=0$ to 5.4 GPa.

netic fields up to 7.5 T. The temperature was determined using a calibrated Cernox sensor which is placed in the compensated region of the superconducting magnet and connected by a Cu heat link directly to the high pressure cell. Here the pressure has been fixed at ambient temperature, but it has also been determined at 4.2 K. Taking the width of the ruby spectra as an indication of the pressure homogeneity in the cell we observed a slight broadening of the ruby line corresponding to pressure gradients of about 4% of the absolute pressure in the cell. Additionally, ac calorimetric experiments under pressure have been performed in a dilution refrigerator for pressures close to 0.5 GPa.

III. RESULTS

The first striking result is obtained in resistivity measurements up to 5.4 GPa (Fig. 2). Clearly, the upturn of the resistivity below T_0 (or T_N at high pressure), which is characteristic of a FS nesting [as produced either by spin density wave (SDW),[34] or a charge density wave (CDW)[35]] is visible in the whole pressure range. It appears much more pronounced than in previous resistivity measurements[36] in the same pressure range and is comparable to recent measurements by Jeffries *et al.*[37] This might be due to the much better hydrostatic pressure conditions. Furthermore, in the previous measurements the resistivity has been measured

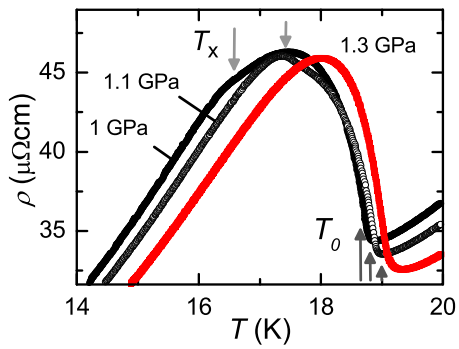

FIG. 3. (Color online) Enlarged view on the resistivity close to the transitions at T_0 (upward arrows) and T_x (downward arrows) for pressures close to P^*. For $P \geqslant 1.3$ GPa the transition at T_x cannot be detected anymore.

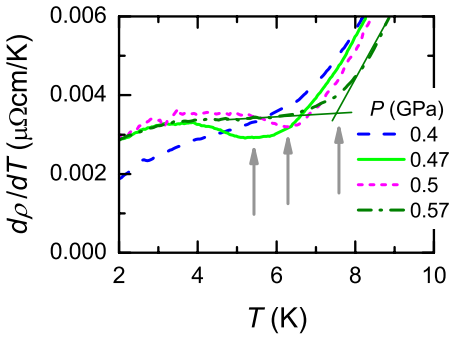

FIG. 4. (Color online) Temperature dependence of the derivative of the resistivity $d\rho/dT$ of URu_2Si_2 for different pressures. A pronounced anomaly develops for $P>0.4$ GPa. The arrows indicate the position of the transition at T_x. The solid lines for $P=0.57$ GPa show the determination of T_x.

with the current along the a axis where the relative jump of the resistivity is less pronounced than along the c axis (almost accomplished in the measurements presented here).[38] However, the resistivity anomaly observed in all pressure ranges implies that the gap opening due to the FS nesting survives in the LMAF phase.

Above $P_x \approx 0.47$ GPa (P_x being the pressure where the transition to the LMAF will be extrapolated at $T=0$ K), a small and broad second anomaly is visible in the resistivity up to $P^* \approx 1.3$ GPa (as shown in Fig. 3). It is more pronounced and therefore better visible in the temperature derivative of the resistivity (Figs. 4 and 5). For $P<0.5$ GPa a clear minimum in the derivative $d\rho/dT$ is observed at T_x (see Fig. 4); on increasing P further, a pronounced shoulder appears in the derivative and T_x is determined by taking a tangent criterion. Starting from P_x the transition temperature T_x shifts to higher temperatures with increasing P and the anomaly at T_x becomes narrower and better defined (Figs. 4 and 5). Above $P^* \approx 1.3$ GPa, where the $T_x(P)$ and $T_0(P)$ lines meet, only one phase transition occurs.

The specific heat detected by the ac technique is presented in Fig. 6 in comparison to the resistivity measurements. The transition at $T_x(P)$ appears as a broadened specific heat

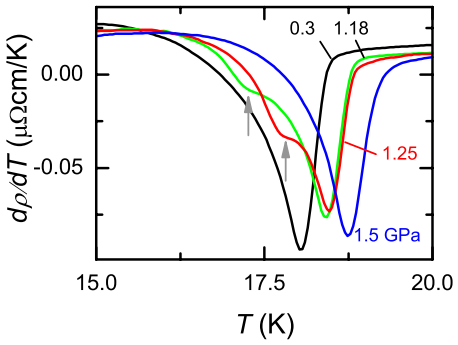

FIG. 5. (Color online) Temperature dependence of the derivative of the resistivity close to the transition of the HO state for different pressures. The arrows indicate the transition at T_x to the LMAF state at $P=1.18$ and 1.25 GPa. No such second anomaly appears for $P>P^*=1.3$ GPa.

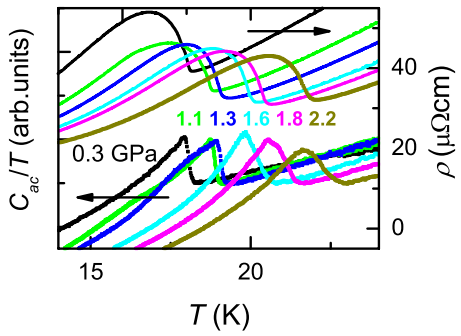

FIG. 6. (Color online) Temperature dependence of specific heat C_{ac}/T (lower data set, left scale) in comparison to the resistivity ρ (upper data, right scale) for different pressures from 0.3 to 2.2 GPa. (Equal colors correspond to equal pressures.)

anomaly which is superimposed on the main specific heat. It is also interesting to observe that above $P^* \approx 1.3$ GPa the main specific heat anomaly at T_N is symmetrical while it is asymmetric in temperature at low pressure at T_0. The change in the shape of the main specific heat anomaly at P^* is also obvious by looking at the normalized width of the transition (Fig. 7). Below 1.3 GPa the width is smaller than 0.5 K, but the behavior changes abruptly for $P > 1.3$ GPa and the transition gets far broader than 1 K. A similar change in regime appears in the P variation of the resistivity anomaly and also in the amplitude of the ratio ρ_{max}/ρ_{min} of the resistivity maxima and minima detected through T_0 or T_N: $P^* = 1.3 \pm 0.05$ GPa (Fig. 8). It is obvious that this phenomenon is not due to the increase of pressure inhomogeneities, but is an intrinsic property of URu_2Si_2.

Another interesting attempt to detect P_x is to look carefully to the P dependence of the electronic scattering as detected by resistivity. First, we will assume the validity of a Fermi liquid law

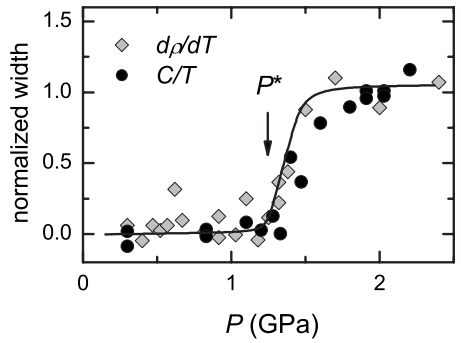

FIG. 7. Normalized width of the phase transition T_0 from resistivity and specific heat measurements. In the resistivity the width is defined by $(T_{min} - T_0)$, T_{min} being the temperature of the minimum of the resistivity at the transition. In the specific heat the width is defined as the difference between the temperatures of the onset and the maximum of the specific heat at the transition. In both quantities the transition broadens for pressures higher than $P^* = 1.3$ GPa. The line is drawn to guide the eye.

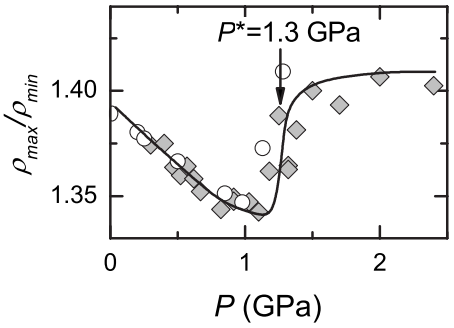

FIG. 8. Height of the resistivity anomaly at the transition T_0 (T_N for $P > 1.3$ GPa) as a function of pressure. The increase of this ratio starting already at $P = 1.1$ GPa is due to the second anomaly at T_x which is on top of the maximum. The arrow indicates the critical pressure P^*. The height of the jump is an indication that part of the Fermi surface is gapped due to nesting which is also observed at high pressure. The line is drawn to guide the eye.

$$\rho = \rho_0 + AT^2$$

for the temperature variation of the resistivity in a limited temperature range from the superconducting transition temperature T_c up to 2.75 K. As shown in Figs. 9(a) and 9(b), P_x is marked by the flattening of the residual resistivity ρ_0 and a maximum of the A coefficient. However, the fit by a T^2 law is rather poor. As used in Ref. 37, a fit of the resistivity taking into account an additional term for an antiferromagnet with a spin excitation gap Δ (see Ref. 39) with

$$\rho = \rho_0 + AT^x + B\frac{T}{\Delta}\left(1 + 2\frac{T}{\Delta}\right)\exp\left(-\frac{\Delta}{T}\right)$$

is only possible with an exponent x as a fifth fitting parameter, which confirms the failure of Fermi liquid behavior just

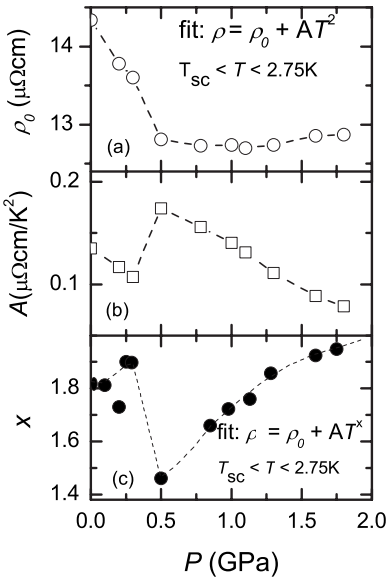

FIG. 9. Pressure dependence of (a) the residual resistivity ρ_0, (b) the A coefficient of the Fermi liquid behavior of the resistivity, and (c) of the resistivity exponent x, obtained by fitting a generalized power law to the low-temperature resistivity.

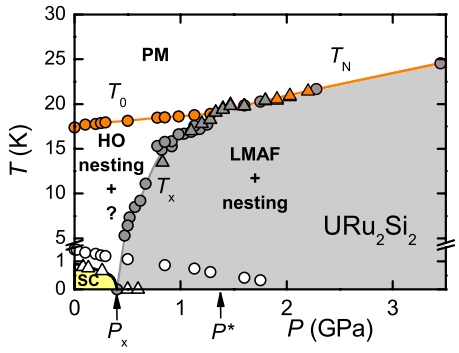

FIG. 10. (Color online) High-pressure phase diagram of URu_2Si_2 from resistivity (circles) and ac calorimetry (triangles). The low-pressure hidden order (HO) state is characterized by a FS nesting which coexists probably with another order parameter. Above P^* only one transition is observed; however, the nesting character of the resistivity is preserved. Bulk superconductivity (SC) detected by ac calorimetry (open triangles) is suppressed when the LMAF state appears. Open circles present the temperature of the onset of the superconducting transition in the electrical resistivity.

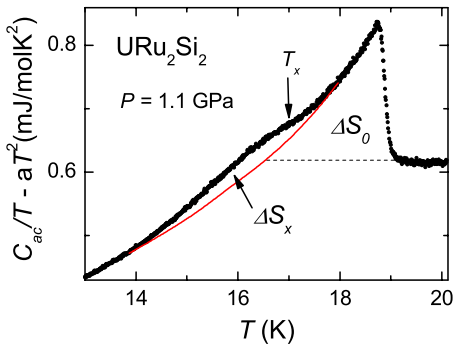

FIG. 11. (Color online) Electronic contribution of the specific heat for $P=1.1$ GPa. The phonon contribution has been determined from a fit $C/T=\gamma+aT^2$ above the transition at T_0. The red curve corresponds to an approximation of the specific heat in the absence of the transition at T_x and has the same shape as C/T at low pressure. ΔS_x (ΔS_0) corresponds to the gain in entropy due to the transition at T_x (T_0), respectively (see the text).

above T_c. It is worthwhile to point out that a similar observation was made at ambient pressure on assumed excellent crystals (see Refs. 40 and 41). Furthermore, due to the observation of the anomaly of the transition to the LMAF state at $T_x(P)$ the temperature range of the validity of this expression is just above P_x very small.

A power law exponent x smaller than 2 is required to represent the data in the temperature range just above T_c. If a parametrization with a generalized power law $\rho=\rho_0+A_xT^x$ is chosen in the temperature range from T_c up to 2.75 K, the exponent x of the power law has a deep minimum with $x=1.4$ just at $P_x=0.5$ GPa [Fig. 9(c)]. The observation that the power law may change drastically in the vicinity of a first-order phase transition at least in a restricted temperature range has been pointed out recently for MnSi (Ref. 42) and $CeRh_2Si_2$ (Ref. 43). If SC would not appear, a T^2 dependence of the resistivity would presumably be obeyed only at very low temperature; its failure in an intermediate temperature range may be caused by multiband effect and the importance of the magnetic contributions.

The phase diagram obtained from the resistivity and ac specific heat measurements is shown in Fig. 10. $T_N(P)$ seems to be the continuation of the $T_x(P)$ line. At low pressure, $T_0(P)$ varies linearly with the slope $\partial T/\partial P=1.01$ K/GPa in good agreement with the variation predicted from thermal expansion[44] and specific heat measurement via the Ehrenfest relation. To point out the contribution at T_x in the specific heat, the electronic and magnetic contribution $C/T-BT^2$ is represented in Fig. 11 at 1.1 GPa. One can see that the suspected first-order transition at T_x from the HO to the LMAF does not correspond to the textbook example of a sudden jump of the entropy at the phase transition but to a broad feature which appears at T_x. This may have a fundamental reason like a weakly first-order transition appearing on top of a regime with strong fluctuations and/or an experimental origin linked to the large sensitivity of the T_x line to pressure and thus to pressure gradients inside the pressure cell. Using the recent results of the volume variation through the T_x and T_0 line $\Delta V_x(T_x)/\Delta V_0(T_0)=10$ (see Ref. 18) associated to a corresponding entropy variation $\Delta S_0(T_0)/\Delta S_x(T_x)\approx 1.6$, one can predict that the pressure dependence of the $T_x(P)$ line is 16 times higher than $T_0(P)$. An extrapolation with a straight line as shown in Fig. 10 gives $\partial T_x/\partial P=10$ K GPa^{-1}, which is roughly the predicted order of magnitude. As it has been already observed in the strain gauge experiment[18] by the strong increase of the thermal expansion at T_N in comparison to the low-pressure signal at T_0, a strong increase of the transition temperature under pressure is observed above P^*.

In contrast to our previous measurements,[45] no indication has been found on cooling of the appearance of first a LMAF transition and then another low-temperature phase with coexisting LMAF and nesting phase for high pressures. Our combined resistivity and specific heat experiments point out the simultaneous coexistence of LMAF with nesting at the transition at T_N. The origin of this discrepancy between the two different experiments can only be explained by the occurrence of an extra weak pressure gradient in our previous experiment due to the change of pressure *in situ* at low temperature. Above 1.3 GPa, at least in both cases, the main calorimetric signature of a phase transition is at T_N; the second one observed on cooling in the previous experiment was only marked by a weak specific heat anomaly. The main order parameter of the high-pressure phase has the characteristics of LMAF with $M_0\approx 0.3\mu_B$ at Q_0. A clear signal in the sublattice magnetization is observed; the NMR spectrum corresponds to a unique LMAF spectrum below T_N.[20]

The pressure variation of the superconducting transition is also drawn in Fig. 10. Let us notice already the difference between the temperature of the onset of superconductivity detected by resistivity ($T_c\approx 1.4$ K) and by specific heat ($T_c\approx 0.8$ K). This indicates that either surface or filament superconductivity, or possibly robust superconductivity in layers near stacking faults, appears at a higher temperature than bulk superconductivity in this tiny URu_2Si_2 crystal. The high sensitivity of superconductivity in URu_2Si_2 to residual im-

perfections is well known.[24,25,30] Even for the best material, a difference of 200 mK in T_C measured by ρ or C is observed and the relatively large broadening of the transition in the resistivity survives even in excellent crystals (see Refs. 30 and 39). In order to learn something about the bulk material properties one has to look at the signal in the specific heat. The interesting point is that the bulk superconductivity anomaly at T_c vanishes above P_x in contrast to the persistence of the onset of superconductivity in the resistivity at least up to 1.8 GPa. This is not astonishing because it does not reflect the bulk property. The width of the superconducting transition in resistivity increases under pressure ($\Delta T_c = 0.15$ K at $P=0$ and $\Delta T_c = 0.29$ K at 1.75 GPa); however, this broadening is negligible compared to the transition width recently reported in Ref. 37. In a previous Grenoble resistivity experiment T_c seems to collapse close to P^*.[45,46] In Ref. 37 it is reported that SC survives even above 1.8 GPa.

In the case of sample inhomogeneities, resistivity, ac susceptibility, and specific heat measurements give different values for T_c. Surprisingly, a good agreement seems to occur in the collapse of the diamagnetic shielding and of the bulk superconductivity at P_x. SC seems to be restricted only to the HO phase and is excluded when a LMAF component exists.[16,47] The intriguing phenomenon is that the disappearance of bulk SC at P_x is clearly coupled to the appearance of LMAF.

IV. DISCUSSION

Contrary to the high sensitivity of the SC properties to imperfections both the T_0 value and the size of the HO specific heat anomaly are robust quantities which are weakly sample dependent.[27] Looking at the presented phase diagram, there is no evidence of a critical end point corresponding to the case A of Ref. 2. Of course, it may happen that the distance of the critical end point to the (T_0, T_N) boundary is too small to be detected experimentally. However, case B with orderings with two order parameters of different symmetry appears likely.

The main argument for the case A scenario is based on the intrinsic origin of the tiny ordered moment below P_x and the excellent description of the inflection point observed in the unusual field dependence of the intensity of the antiferromagnetic Bragg reflection at Q_0.[48] However, today the detection of the tiny ordered moment M_0 below P_x appears most probably as a parasitic effect caused by imperfections. Thus, the tiny ordered moment may not be an intrinsic property at low pressures but it comes certainly from the high-pressure sensitivity of the pure material (low value of P_x). Notably, near stacking defaults where large pressure gradients of few tens of GPa over atomic distances can be induced, small droplets of the LMAF phase can be nucleated (that may be also true for residual HO droplets above P_x and thus the origin of the residual superconductivity discussed above). Detailed neutron scattering experiments under uniaxial stress have pointed out that the low-temperature state of URu_2Si_2 is extremely sensitive to small strain effects.[49] Recent careful and systematic neutron diffraction experiments[16] derive a $T_x(P)$ line through the emergence of the large sublattice magnetization, which is in very good agreement with the one drawn in Fig. 10. In these new measurements, the residual ordered moment M_0 in the HO is less than $0.01\mu_B$. Additionally, the temperature of the onset of the magnetic intensity at 13.5 K is even far less than T_0 of the HO state;[16] a clear inhomogeneity occurs in the material assumed to be of high quality from the low residual value of M_0 at ambient pressure compared to previous measurements[27] where annealing has led to the coincidence between the appearance of tiny sublattice magnetization and the HO phase transition at T_0.

As developed in theoretical models,[50,51] the unusual phase diagram of URu_2Si_2 has its origin in the duality between the itinerant and localized nature of the $5f$ electrons. For U ions in a metallic environment, valence fluctuations occur between the $U^{3+}(5f^3)$ and $U^{4+}(5f^2)$ configurations; pressure must favor a final $5f^2$ configuration, which is rather similar to the $4f^2$ situation of Pr, well known to present often a singlet crystal-field ground state and associated phenomena such as a magnetic ordering for a critical value of the exchange interactions.[52]

For the heavy fermion compound UPd_2Al_3 a duality model of localized and itinerant $5f$ electrons has been proposed,[53] where the localized part corresponds to a $5f^2$ configuration and the itinerant part to an extra $5f$ electron. In the same spirit, studies of $4f$ intermediate valence systems such as TmSe have shown that even if the valence is intermediate, the local magnetism may be renormalized to the 2^+ or 3^+ configuration.[32] A simple picture to understand the complex phase diagram of URu_2Si_2 is to assume a competition between two different ground states corresponding, for example, to a spin density wave (SDW) at the incommensurate wave vector Q_1 and to LMAF at the commensurate wave vector Q_0.

The possibility that the HO phase is a SDW with Q_1 wave vector is suggested by the inelastic magnetic neutron scattering response. Indeed, a drastic change occurs in the inelastic neutron spectrum[9–11] at T_0 with the formation of a characteristic energy gap $E_1 \sim 4.2$ meV at Q_1. Furthermore, the evolution of the inelastic contribution can well explain the drop of entropy below T_0.[9] However, below P_x the assignment of the HO to a SDW with a wave vector Q_1 is yet not established. If the ordering is due to dipole moments it may influence the NMR signal but no sign of a spin-density wave has been reported yet even in very recent careful NMR measurements.[21] This suggests that the FS nesting is associated to a more complex order parameter (e.g., octupole ordering).

The real order parameter of the HO may be much more complex than a SDW. However, if for the best crystal no sublattice magnetization M_0 may appear at low pressure in the HO phase,[16,20–22] the energy spectrum at the commensurate wave vector Q_0 and its temperature dependence is a very robust quantity independent of the size of M_0. All measurements show a clear energy gap at $E_0 = 2.1$ meV while above T_0 the spectrum becomes quasielastic ($E_0 = 0$) and its intensity will collapse above 25 K. The temperature evolution of the spectrum at Q_1 above T_0 is different as the excitation remains inelastic but strongly damped.[9–11] As the temperature variation of the intensities of the spectrum at E_0 for Q_0

and at E_1 for Q_1 can be superimposed below T_0, the simple idea is that the gap opening at Q_1 corresponds to a drop of the density of states at the Fermi level. The feedback of lowering the carrier number below T_0 is a decrease of the magnetic fluctuations around Q_0. That leads one to recover a spectrum characteristic of a $5f^2$ configuration with a well resolved crystal-field excitation at E_0. An illustrating example of a gap opening on an inelastic spectrum characteristic of a local magnetism is well established for superconductivity (see the recent experiment[54] on $PrOs_4Sb_{12}$). This has also recently been observed in the skutterudite system $PrFe_4P_{12}$, where an interplay between a nesting and a complex multipolar ordering appears.[55,56] To summarize, we point out the mutual influence between the formation of a ground-state characteristic of the itinerant contribution (Q_1, E_1) and the emergence of a localized behavior (Q_0, E_0) even in the absence of LMAF.

Increasing the pressure just above P_x at $P_x+\varepsilon$ leads to a situation where, in a large temperature interval from T_0 to T_x, a concomitant formation of energy gap occurs at E_1 and E_0 for Q_1 and Q_0; thus little magnetic entropy is left at the phase transition T_x. The $T_x(P)$ line is dominated by the volume and sublattice magnetization jump. Of course just below the critical point $P^*-\varepsilon$, when T reaches T_x the gap at E_0 and E_1 is not fully opened, and the entropy variation at T_x becomes large as shown in Fig. 11. Entering in the LMAF phase, the inelastic neutron spectrum at Q_0 seems to be modified and the characteristic gap energy[57,58] collapses. Such behavior is at least in good qualitative agreement with the evolution of the collective excitations in magnetically ordered materials with a singlet crystal-field ground state.[50,59] In contrast, the gap at Q_1 is very robust and increases with P like T_N. The establishment of LMAF at T_N requires the restoration of a $5f^2$-like local magnetism and thus the concomitant opening of a gap with energy E_1 at Q_1 to allow a slow localized moment regime. An appealing proposal is that below P_x the ordering is mainly driven by the nesting at Q_1 and above P^* by the LMAF phase at Q_0. At high pressures a change in the inelastic spectrum at Q_1 is required in order to preserve the condition of a low carrier density and to reach the regime of slow spin fluctuations. Comparing different NMR results[20,60] supports the conclusion of a strong drop of the nuclear relaxation time at T_0 and T_N, i.e., on both sides of P_x.

The occurrence of superconductivity is clearly forbidden in the LMAF phase where $M_0=0.3\mu_B$ and E_0 collapses. The coexistence of AF and SC in heavy fermion compounds is still not fully understood.[61] For example, UPd_2Al_3 is a case where AF and SC coexist peacefully like in Chevrel phases or borocarbides which are conventional antiferromagnetic systems with different electronic baths responsible for SC and magnetic properties. There are other examples such as $CeCu_2Si_2$, $CeRhIn_5$, $CeRhSi_3$, and $CeIrSi_3$ where a coexisting domain is either excluded or restricted to a narrow pressure range around the condition $(T_N \sim T_c)$.[61]

There is no microscopic indication on the origin of the residual inhomogeneous SC above P_x. At the opposite to the case of $ZrZn_2$,[62] we have verified that the origin is not coming from surface effects due to sample cutting as in previous work it survives through annealing and chemical treatments. The possibility of an impurity phase as Ru in Sr_2RuO_4 seems also unlikely[63] because at least at $P=0$ all reported measurements show a drop in the resistivity roughly 200 mK above the T_c derived from specific heat. An interesting possibility is that this residual SC is generated near defects characteristic of the URu_2Si_2 lattice; thus residual LMAF and SC on both sides of P_x may have the same origin. As URu_2Si_2 crystals can be cleaved nicely with a beautiful basal plane surface, it would certainly be possible to get information by scanning tunneling microscopy. The high sensitivity of URu_2Si_2 to uniaxial stress is illustrated by the opposite sign in the thermal linear expansion measured along the c and a axes at the successive phase transition at T_0 and T_c.[44,64] It is interesting to remark that for SC a similar effect is observed in the case of $CeIrIn_5$,[65] where resistivity measurements indicate T_c above 1 K while specific heat gives clearly T_c equal to 0.4 K.

V. SUMMARY

The high-pressure phase diagram of the heavy fermion compound URu_2Si_2 has been studied by resistivity and specific heat experiment under highly hydrostatic conditions. In both quantities we could observe the transition line from the hidden order state at low pressure to the large moment antiferromagnetic phase at high pressure. This transition line $T_x(P)$ seems to join the transition line of the hidden order $T_0(P)$ at $P^* \sim 1.3$ GPa. Our resistivity measurements clearly show that the nesting behavior characteristic for the HO state at low pressure is preserved up to the highest pressure $P=5.4$ GPa. The high-pressure LMAF coexists with at least a dynamical nesting. A possible route to understand the pressure-temperature phase diagram is given by the duality picture of the $5f$ uranium electrons. Below P^* the HO is dominated by nesting properties of the itinerant electrons with strong feedback on the localized part and vice versa at high pressures. An uncertainty remains on the relative symmetry of the two coexisting orderings and thus the fascinating point remains the nature of the HO phase.

ACKNOWLEDGMENTS

This work has been supported by the ANR programmes ICENET and ECCE. E.H. acknowledges financial support by EGIDE. The authors thank F. Bourdarot, V. P. Mineev, K. Miyake, and M. E. Zhitomirsky for stimulating discussions and critical reading of the manuscript. We are grateful to A. Demuer for help in sample preparation for the high-pressure experiment.

*elena.hassinger@cea.fr

[1] C. Broholm, J. K. Kjems, W. J. L. Buyers, P. Matthews, T. T. M. Palstra, A. A. Menovsky, and J. A. Mydosh, Phys. Rev. Lett. **58**, 1467 (1987).
[2] V. P. Mineev and M. E. Zhitomirsky, Phys. Rev. B **72**, 014432 (2005).
[3] P. Santini and G. Amoretti, Phys. Rev. Lett. **73**, 1027 (1994).
[4] F. J. Ohkawa and H. Shimizu, J. Phys.: Condens. Matter **11**, L519 (1999).
[5] A. Kiss and P. Fazekas, Phys. Rev. B **71**, 054415 (2005).
[6] P. Chandra, P. Coleman, J. A. Mydosh, and V. Tripathi, Nature (London) **417**, 831 (2002).
[7] C. M. Varma and L. Zhu, Phys. Rev. Lett. **96**, 036405 (2006).
[8] N. H. van Dijk, F. Bourdarot, J. C. P. Klaasse, I. H. Hagmusa, E. Brück, and A. A. Menovsky, Phys. Rev. B **56**, 14493 (1997).
[9] C. R. Wiebe, J. A. Janik, G. J. MacDougall, G. M. Luke, J. D. Garrett, H. D. Zhou, Y.-J. Yo, L. Belicas, Y. Qiu, J. R. D. Copley, and W. J. L. Buyers, Nat. Phys. **3**, 96 (2007).
[10] C. Broholm, H. Lin, P. T. Matthews, T. E. Mason, W. J. L. Buyers, M. F. Collins, A. A. Menovsky, J. A. Mydosh, and J. K. Kjems, Phys. Rev. B **43**, 12809 (1991).
[11] F. Bourdarot, Ph.D. thesis, University Joseph Fourier, Grenoble, 1993.
[12] M. B. Maple, J. W. Chen, Y. Dalichaouch, T. Kohara, C. Rossel, M. S. Torikachvili, M. W. McElfresh, and J. D. Thompson, Phys. Rev. Lett. **56**, 185 (1986).
[13] J. Schoenes, C. Schönenberger, J. J. M. Franse, and A. A. Menovsky, Phys. Rev. B **35**, 5375 (1987).
[14] K. Behnia, R. Bel, Y. Kasahara, Y. Nakajima, H. Jin, H. Aubin, K. Izawa, Y. Matsuda, J. Flouquet, Y. Haga, Y. Onuki, and P. Lejay, Phys. Rev. Lett. **94**, 156405 (2005).
[15] P. A. Sharma, N. Harrison, M. Jaime, Y. S. Oh, K. H. Kim, C. D. Batista, H. Amitsuka, and J. A. Mydosh, Phys. Rev. Lett. **97**, 156401 (2006).
[16] H. Amitsuka, K. Matsuda, I. Kawasaki, K. Tenya, M. Yokoyama, C. Sekine, N. Tateiwa, T. C. Kobayashi, S. Kawarazaki, and H. Yoshizawa, J. Magn. Magn. Mater. **310**, 214 (2007).
[17] H. Amitsuka, M. Sato, N. Metoki, M. Yokoyama, K. Kuwahara, T. Sakakibara, H. Moromoto, S. Karawazaki, Y. Miyako, and J. A. Mydosh, Phys. Rev. Lett. **83**, 5114 (1999).
[18] G. Motoyama, T. Nishioka, and N. K. Sato, Phys. Rev. Lett. **90**, 166402 (2003).
[19] F. Bourdarot, B. Fåk, V. P. Mineev, M. E. Zhitomirsky, N. Kernavanois, S. Raymond, F. Lapierre, P. Lejay, and J. Flouquet, Physica B **350**, e179 (2004); F. Bourdarot, A. Bombardi, P. Burlet, M. Enderle, J. Flouquet, N. Kernavanois, V. P. Mineev, L. Paolasini, M. E. Zhitomirsky, and B. Fåk, *ibid.* **359-361**, 986 (2005).
[20] K. Matsuda, Y. Kohori, T. Kohara, K. Kuwahara, and H. Amitsuka, Phys. Rev. Lett. **87**, 087203 (2001).
[21] S. Takagi, S. Ishihara, S. Saitoh, H. Sasaki, H. Tanida, M. Yokoyama, and H. Amitsuka, J. Phys. Soc. Jpn. **76**, 033708 (2007).
[22] A. Amato, M. J. Graf, A. de Visser, H. Amitsuka, D. Andreica, and A. Schenck, J. Phys.: Condens. Matter **16**, S4403 (2004).
[23] W. Schlabitz, J. Baumann, B. Pollit, U. Rauchschwalbe, H. M. Mayer, U. Ahlheim, and C. D. Bredl, Z. Phys. B: Condens. Matter **62**, 171 (1986).
[24] A. P. Ramirez, T. Siegrist, T. T. M. Palstra, J. D. Garrett, E. Bruck, A. A. Menovsky, and J. A. Mydosh, Phys. Rev. B **44**, 5392 (1991).
[25] K. Hasselbach, P. Lejay, and F. Flouquet, Phys. Lett. A **156**, 313 (1991).
[26] J. P. Brison, N. Keller, A. Vernièr, P. Lejay, L. Schmidt, A. Buzdin, J. Flouquet, S. R. Julien, and G. G. Lonzarich, Physica C **256**, 128 (1995).
[27] B. Fak, C. Vettier, J. Flouquet, F. Bourdarot, S. Raymond, A. Vernièr, P. Lejay, P. Boutrouille, N. R. Bernhoeft, S. T. Bramwell, R. A. Fisher, and N. E. Phillips, J. Magn. Magn. Mater. **154**, 339 (1996).
[28] C. Bergemann, S. R. Julien, G. L. McMullan, B. K. Howard, P. Lejay, J. P. Brison, and J. Flouquet, Physica B **230-232**, 348 (1997).
[29] Y. S. Oh, Kee Hoon Kim, P. A. Sharma, N. Harrison, A. Amitsuka, and J. A. Mydosh, Phys. Rev. Lett. **98**, 016401 (2007).
[30] K. Hasselbach, Ph.D. thesis, University of Karlsruhe, 1991.
[31] A. Demuer, C. Marcenat, J. Thomasson, C. Calemczuk, B. Salce, P. Lejay, D. Baithwaite, and J. Flouquet, J. Low Temp. Phys. **120**, 245 (2000).
[32] J. Derr, G. Knebel, G. Lapertot, B. Salce, M.-A. Méasson, and J. Flouquet, J. Phys.: Condens. Matter **18**, 2089 (2006).
[33] B. Salce, J. Thomasson, A. Demuer, J. J. Blanchard, J. M. Martinod, L. Devoille, and A. Guillaume, Rev. Sci. Instrum. **71**, 2461 (2000).
[34] E. Fawcett, Rev. Mod. Phys. **60**, 209 (1988).
[35] See *Charge Density Waves in Solids*, edited by L. P. Gor'kov and G. Grüner (North-Holland, Amsterdam, 1989).
[36] G. Oomi, T. Kagayama, Y. Onuki, and T. Komatsubara, Physica B **199&200**, 148 (1994).
[37] J. R. Jeffries, N. P. Butch, B. T. Yukich, and M. B. Maple, Phys. Rev. Lett. **99**, 217207 (2007).
[38] T. T. M. Palstra, A. A. Menovsky, and J. A. Mydosh, Phys. Rev. B **33**, 6527 (1986).
[39] N. H. Andersen, in *Crystalline Electric Field and Structural Effects in f-Electron Systems*, edited by J. E. Crow, R. P. Guertin, and T. W. Mihalisin (Plenum, New York, 1980), p. 373.
[40] Y. Kasahara, T. Iwasawa, H. Shishido, T. Shibauchi, K. Behnia, Y. Haga, T. D. Matsuda, Y. Onuki, M. Sigrist, and Y. Matsuda, Phys. Rev. Lett. **99**, 116402 (2007).
[41] Y. Haga (private communication).
[42] N. Doiron-Leyraud, I. R. Walker, L. Taillefer, M. J. Steiner, S. R. Julien, and G. G. Lonzarich, Nature (London) **425**, 595 (2003).
[43] R. Boursier, Ph.D. thesis, University Joseph Fourier, Grenoble, 2005.
[44] A. de Visser, F. E. Kayzel, A. A. Menovsky, J. J. M. Franse, J. van den Berg, and G. J. Nieuwenhuys, Phys. Rev. B **34**, 8168 (1986).
[45] G. Knebel, K. Izawa, F. Bourdarot, E. Hassinger, B. Salce, D. Aoki, and F. Flouquet, J. Magn. Magn. Mater. **195-200**, 310 (2007).
[46] L. Schmidt, Ph.D. thesis, University Joseph Fourier, Grenoble, 1993.
[47] N. K. Sato, S. Uemura, G. Motoyama, and T. Nishioka, Physica B **378-380**, 378 (2006).
[48] F. Bourdarot, B. Fåk, K. Habicht, and K. Prokes, Phys. Rev. Lett. **90**, 067203 (2003).
[49] M. Yokoyama, H. Amitsuka, K. Tenya, K. Watanabe, S. Kawarazaki, H. Yoshizawa, and J. A. Mydosh, Phys. Rev. B **72**, 214419 (2005).
[50] A. E. Sikkema, W. J. L. Buyers, I. Affleck, and J. Gan, Phys. Rev.

B **54**, 9322 (1996).
[51] Y. Okuno, J. Phys. Soc. Jpn. **67**, 2469 (1998).
[52] Y. L. Wang and B. R. Cooper, Phys. Rev. **185**, 696 (1969).
[53] N. K. Sato, N. Aso, K. Miyake, R. Shiina, P. Thalmeier, G. Varelogianis, C. Geibel, F. Steglich, P. Fulde, and T. Komatsubara, Nature (London) **410**, 340 (2001).
[54] K. Kuwahara, K. Iwasa, M. Kohgi, K. Kaneko, N. Metoki, S. Raymond, M.-A. Méasson, J. Flouquet, H. Sugawara, Y. Aoki, and H. Sato, Phys. Rev. Lett. **95**, 107003 (2005).
[55] J. Kikuchi, M. Takigawa, H. Sugawara, and H. Sato, J. Phys. Soc. Jpn. **76**, 043705 (2007).
[56] H. Harima and K. Takegahara, Physica B **312-313**, 843 (2002).
[57] F. Bourdarot, B. Fåk, V. P. Mineev, M. E. Zhitomirsky, N. Kernavanois, S. Raymond, P. Burlet, F. Lappiere, P. Lejay, and J. Flouquet, arXiv:cond-mat/0312206 (unpublished).
[58] A. Villaume, F. Bourdarot, E. Hassinger, S. Raymond, D. Aoki, and J. Flouquet (to be published).
[59] Y. L. Wang and B. R. Cooper, Phys. Rev. **172**, 539 (1968).
[60] T. Kohara, Y. Kohori, K. Asayama, Y. Kitaoka, M. B. Maple, and M. S. Torikachvili, Solid State Commun. **59**, 603 (1986).
[61] See J. Flouquet, in *Progress in Low Temperature Physics*, edited by W. P. Halperin (Elsevier, Amsterdam, 2006), Vol. XV, p. 139.
[62] E. A. Yelland, S. M. Hayden, S. J. C. Yates, C. Pfleiderer, M. Uhlarz, R. Vollmer, H. v. Löhneysen, N. R. Bernhoeft, R. P. Smith, S. S. Saxena, and N. Kimura, Phys. Rev. B **72**, 214523 (2005).
[63] H. Yaguchi, M. Wada, T. Akima, Y. Maeno, and T. Ishiguro, Phys. Rev. B **67**, 214519 (2003).
[64] N. H. Van Dijk, A. de Visser, J. J. M. Franse, and A. A. Menovsky, Phys. Rev. B **51**, 12665 (1995).
[65] N. Oeschler, P. Gegenwart, R. Movshovich, J. L. Sarrao, J. D. Thompson, and F. Steglich, Phys. Rev. Lett. **91**, 076402 (2003).